Total ionizing dose effect of γ-ray radiation on the switching characteristics and filament stability of HfOx resistive random access memory

Runchen Fang,[1,2] Yago Gonzalez Velo,[2] Wenhao Chen,[2] Keith E. Holbert,[2] Michael N. Kozicki,[2] Hugh Barnaby,[2] and Shimeng Yu[1,2,a)]

[1]*School of Computing, Informatics, and Decision Systems Engineering, Arizona State University, Tempe, Arizona 85281, USA*

[2]*School of Electrical, Computer, and Energy Engineering, Arizona State University, Tempe, Arizona 85287, USA*

(Received 8 March 2014; accepted 27 April 2014; published online 7 May 2014)

The total ionizing dose (TID) effect of gamma-ray (γ-ray) irradiation on HfOx based resistive random access memory was investigated by electrical and material characterizations. The memory states can sustain TID level ~5.2 Mrad (HfO_2) without significant change in the functionality or the switching characteristics under pulse cycling. However, the stability of the filament is weakened after irradiation as memory states are more vulnerable to flipping under the electrical stress. X-ray photoelectron spectroscopy was performed to ascertain the physical mechanism of the stability degradation, which is attributed to the Hf-O bond breaking by the high-energy γ-ray exposure. © *2014 AIP Publishing LLC*. [http://dx.doi.org/10.1063/1.4875748]

The resistive switching phenomenon in metal oxides is intriguing and has initiated the development of the resistive random access memory (RRAM) technology for the next generation of non-volatile memory (NVM) beyond the FLASH technology.[1–3] HfOx-based RRAM devices have demonstrated great scalability (<10 nm), fast switching speed (<10 ns), low energy consumption (<pJ/bit), good reliability (>10^{10} cycles and >10 yr extrapolated at 85 °C), multi-bit capability, and compatibility with complementary metal oxide semiconductor (CMOS) technology.[4–6] The RRAM switching mechanism between the low resistance state (LRS) and the high resistance state (HRS) is generally attributed to the formation and rupture of the conductive filament which may consist of oxygen vacancies.[7–9] For aerospace applications, the lack of low-cost high-density radiation-hardened NVM is a severely limiting factor in the design of systems for the harsh space environment. Present solutions relying on FLASH technology can only sustain a total ionizing dose (TID) up to 75 krad (Si).[10] Therefore, it is necessary to assess the radiation hardness of the emerging memory technologies such as RRAM as alternatives for FLASH. In this work, we report the results of a gamma-ray (γ-ray) irradiation study on the HfOx-based RRAM devices showing TID hardness ~5.2 Mrad (HfO_2) and we also analyze the physical mechanism of degraded filament stability.

Generally, there are five types of radiation sources employed in laboratory testing: Photons (x-ray, γ-ray), electrons, light ions (protons, α-particles), heavy ions, and neutrons. For TiOx, TaOx, NiOx, based RRAM, Cu doped HfOx, and chalcogenide based programmable metallization cells (PMC), radiation effects have been studied with various radiation sources.[11–23] For the Cu doped HfOx RRAM in Ref. 22, the switching mechanism was attributed to the Cu ion migration and formation/rupture of Cu filament, while in this work, the switching mechanism was attributed to the generation/recombination of oxygen vacancies.[8] For the HfOx-based RRAM with oxygen vacancy filament, there were reports on X-ray[19] and the heavy ion[18] radiation effects but no report on the γ-ray radiation effect. As HfOx is the one of the most mature RRAM materials[4–6] and the highly penetrating γ-rays do not cause other phenomena such as displacement damage and nuclear reactions, it is prudent to perform a TID effect study using γ-ray on the HfOx device.

RRAM devices with a structure of TiN(50 nm)/HfOx(10 nm)/Pt(50 nm) were fabricated by e-beam evaporator deposition of Pt films on the silicon oxide substrate as the bottom electrode, atomic layer deposition (ALD) of HfOx using TEMA-Hf and H_2O as precursors at 220 °C, and reactive sputtering of TiN as the top electrode. The details of the switching characteristics were reported in Ref. 24. The DC sweep and electrical stress of the RRAM devices were measured using a Keithley 4200 semiconductor parameter analyzer. The pulse cycling responses of the RRAM devices were tested with an Agilent 81160A pulse generator. A batch of HfOx RRAM devices were exposed to ^{60}Co γ-rays (1.25 MeV) at a dose-rate of 557 rad(HfO_2)/min in a Gammacell 220 irradiator to observe the step-radiation and total ionizing dose effects. X-ray photoelectron spectroscopy (XPS) was performed on pre- and post- irradiation samples with a Vacuum Generator, Escalab 220i-XL.

The typical DC sweep responses of the HfOx based RRAM devices are shown in Figure 1(a). The devices are functional after a ~6 V forming process. To set the devices from the HRS to the LRS, a positive voltage sweep from 0 V to 2 V is used with a current compliance of 100 μA, and to reset the devices from the LRS to the HRS, a negative voltage sweep from 0 to −2.3 V is used. The typical pulse cycling of 5 different devices with an active area of $5 \times 5\ \mu m^2$ is shown in Figure 1(b). A positive pulse of 2 V/50 ns was applied to set the devices to the LRS and a negative pulse of −2.7 V/50 ns was applied to reset the devices to the HRS.

In order to examine the effects of radiation on the data retention, the resistance evolution was tracked on 60 samples

a)Email: shimengy@asu.edu

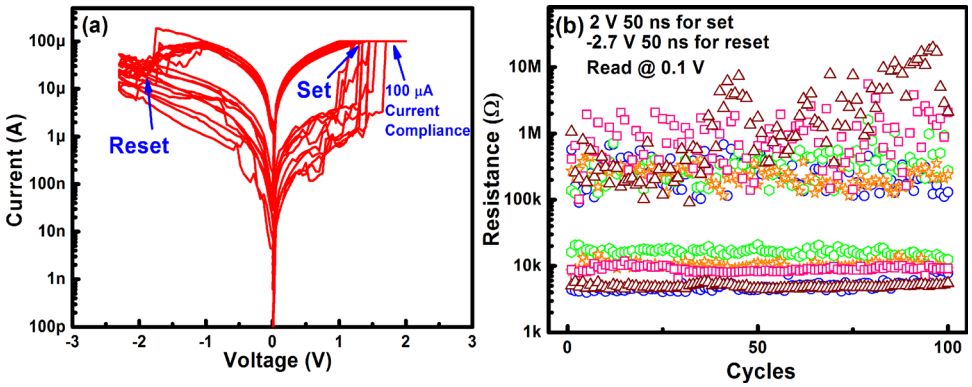

FIG. 1. (a) Typical I-V curves of the resistive switching behaviors of the TiN/HfOx/Pt RRAM devices and (b) pulse cycling of five different devices with an area of $5 \times 5\ \mu m^2$.

with different active areas, $0.5 \times 0.5\ \mu m^2$, $1 \times 1\ \mu m^2$, and $5 \times 5\ \mu m^2$ (20 samples for each size). Before irradiation, different values of resistances covering a full range from the LRS to the HRS (~4 kΩ to ~100 MΩ) were deliberately programmed to include different filament shapes or gaps (where the material is deficient in oxygen vacancies). Figure 2(a) shows the evolution of resistance states of five different devices with an active area of $5 \times 5\ \mu m^2$ along with increasing γ-ray dose. The samples were taken out of the radiation source to perform the resistance value check by applying a 0.1 V read voltage immediately (within 1.5 h) after exposure. The devices were then put back in the radiation source. The resistance values remained almost constant after the 5.2 Mrad (HfO_2) dose except the high resistance values decreased slightly, nevertheless, the memory window is still well maintained. Figure 2(b) shows the resistance comparison of all the 60 samples between pre-irradiation and post-irradiation. It is seen that the resistance values before and after the exposure are almost the same (as indicated by a line with a slope of 1 in this graph), suggesting that the γ-ray irradiation does not affect the memory states, and thus the filament shape does not change significantly.

After the 5.2 Mrad (HfO_2) γ-ray dose, the pulse cycling of the irradiated samples and the control samples was tested using the same pulse condition (2 V/50 ns for set and −2.7 V/50 ns for reset). Statistics of the resistance distribution obtained for 100 pulse cycles for pre- and post-irradiation samples with three different active areas (5 cells in each size) are shown in Figure 3(a). The general trend is that for larger area cells, the HRS value is smaller (similar as shown in Ref. 4). If we compare the pre- and post-irradiation data for each size, the average HRS value decreases slightly after the exposure and the LRS value remains almost the same, indicating that more oxygen vacancies are generated in the non-filament region in the irradiated samples which may contribute to more leakage current in the HRS. Moreover, we examined the DC performance of 15 devices after irradiation including the initial state, forming voltage, set voltage, and reset voltage distributions. The distribution of set voltage and reset voltage before and after irradiation is shown in Figure 3(b). The initial state, forming voltage slightly decrease, and set voltage almost keeps the same after irradiation. However, reset voltage decreased about 0.4 V after irradiation.

In addition, the electrical stress response was measured, and the result is shown in Figure 4. For the control samples, the LRS can withstand 10^4 s with the highest constant bias of −1.1 V, and the HRS can withstand 10^4 s with the highest constant bias of 0.9 V. However, for the irradiated samples, the HRS can be maintained for several thousand seconds only under the constant bias of 0.9 V, and then, it switches to the LRS. The LRS could not even sustain several tens of seconds under the constant bias of −1.1 V until it switches to the HRS. This suggests that the filament stability is

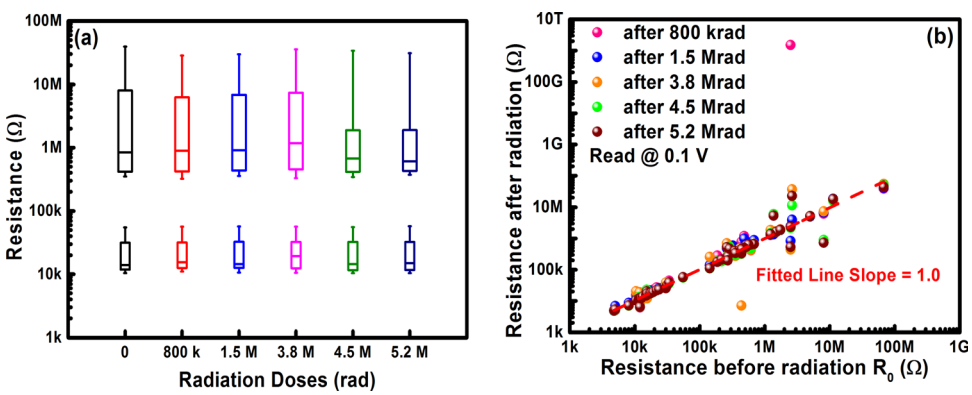

FIG. 2. (a) Resistance states evolution with different γ-ray doses for 20 samples of $5 \times 5\ \mu m^2$ (the upper edge of the box shows the 75% of the distribution, and lower edge shows the 25% of the distribution). (b) Resistance comparison before and after irradiation for all the 60 samples.

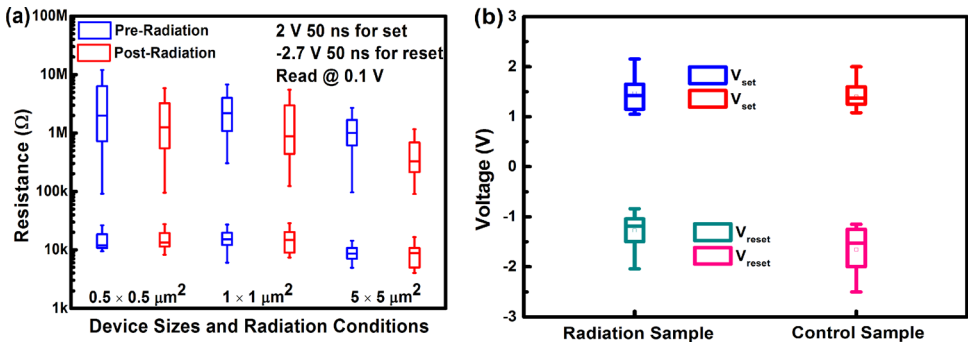

FIG. 3. (a) Statistics of resistance distribution by pulse cycling of the control samples and the irradiated samples. (b) The distribution of set voltage and reset voltage before and after irradiation. The statistics were obtained from devices with three different areas and each area includes 5 different devices (the upper edge of the box shows the 75% of the distribution, and lower edge shows the 25% of the distribution, and the square shows the mean value of the distribution).

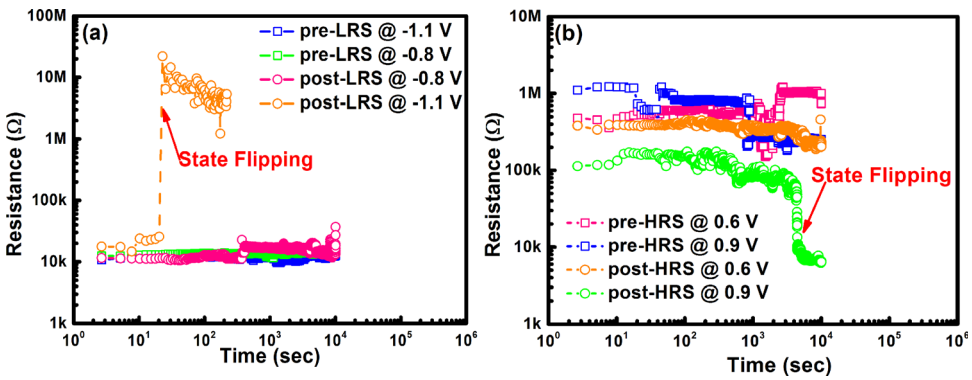

FIG. 4. The 10^4 s electrical stress on the control samples and the radiation samples with constant bias of (a) −0.8 V and −1.1 V on the LRS and (b) 0.6 V and 0.9 V on the HRS.

weakened after the radiation. This observation of unstable filament (especially in the LRS) at high voltage stress after γ-ray irradiation is consistent with the reset voltage reduction after γ-ray irradiation in Figure 3(b).

In order to gain more insight into the physical mechanism of γ-ray radiation effects on the HfOx RRAM devices, XPS was performed on the control and irradiated samples. The XPS depth sensitivity is about 5 nm, thus the information from the sample surface down to 5 nm deep region was collected. In Figure 5(a), the O 1s peaks show that the O-Hf bonds are located around 530 eV and other non-bridging oxygen bonds are located around 532 eV.[25] The area ratio of O-Hf bonds to non-bridging oxygen bonds changed from 7:1 to 2.6:1 which indicates that the amount of non-bridging oxygen at the surface of the HfOx has increased after irradiation. Figure 5(b) shows the Hf 4f peaks from the XPS. An obvious shift of 0.6 eV of the two Hf 4f half peaks 4f5/2 and 4f7/2 to higher energy level is observed, indicating the reduction of the valence of the Hf element.[26] The reduction in valence of the Hf element also agrees with the fact of O-Hf bond breaking.

The key observations from the above experiments include that (1) the HRS and LRS resistance values do not change significantly after the γ-ray radiation, indicating that

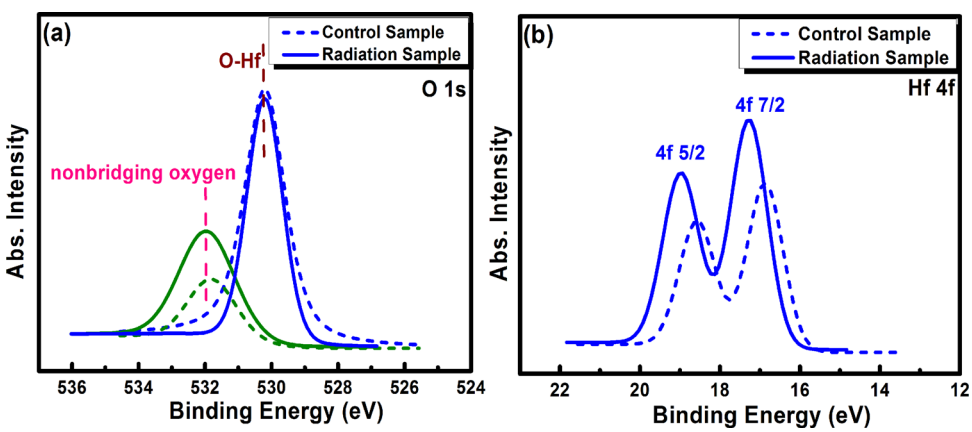

FIG. 5. The XPS spectrum of (a) O 1s and (b) Hf 4f peaks of the control and irradiated samples.

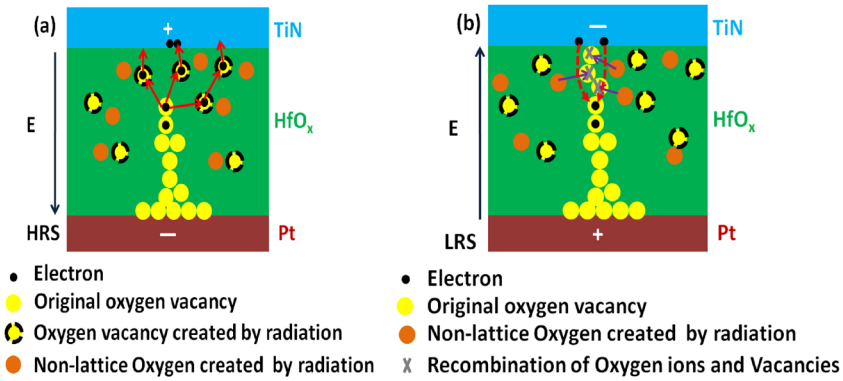

FIG. 6. Schematic of the physical mechanism that illustrates the γ-ray radiation effect on the RRAM cell in (a) the HRS and (b) the LRS (Red line means the electron transport path, and purple line means the oxygen migration path).

the filament shape may not change as well; (2) the HRS resistance in the pulse cycling decreases slightly after the γ-ray irradiation, indicating more oxygen vacancies generated in the non-filament region; (3) the maximum voltage stress that the device can sustain and the reset voltage decrease after irradiation, indicating the stability of the filament becomes weakened; (4) more non-bridging oxygen bonds show up after irradiation, indicating that high energy γ-rays may break up the Hf-O bonds.

Based on these observations, we propose in Figure 6 physical picture to illustrate how γ-rays exposures may affect HfOx RRAM characteristics. That is, high energy γ-rays break up some of the Hf-O bonds, which may result in the oxygen vacancies and non-lattice oxygen in interstitial sites. The shape of the filament in the LRS or the residual filament in the HRS is not affected noticeably as the amount of the newly generated oxygen vacancies is small as compared with those in the filament region. Therefore, the LRS and HRS resistance states do not change significantly after radiation exposure. However, in the subsequent pulse cycling or DC sweep operations, there are more oxygen vacancies present in the bulk, thus the average HRS resistance decreases slightly as those oxygen vacancies far away from the filament region are not recovered during the reset process. Although the shape of the filament does not change substantially, the stability of the filament in the LRS or the residual filament in the HRS is weakened. In the HRS, in the gap region, there are more oxygen vacancies that help to reconnect the filament under the set operation electrical stress (Figure 6(a)). In the LRS, there are even more non-lattice oxygen around the filament region that can migrate towards the filament to rupture the filament easily under the reset operation electrical stress (Figure 6(b)).

In summary, the TID effect from γ-ray irradiation on the HfOx based RRAM was investigated by electrical and material characterizations. The memory states are sustained after a total ionizing dose of 5.2 Mrad (HfO_2) without significant change in the functionality or the switching characteristics under pulse cycling. However, the stability of the filament is weakened after irradiation as memory states are more vulnerable to flipping under the electrical stress. The physical mechanism of the stability degradation is attributed to the Hf-O bond breaking as indicated by the XPS study. Our work extends the understanding of the effects of ionizing radiation on oxide based RRAM in general and can guide the design of oxide based RRAM for aerospace applications.

The authors would like to thank Herbert Bowler of Arizona State University for the irradiation support in the research. This work funded by the Defense Threat Reduction Agency (DTRA) under Grant HDTRA1-11-1-0055. The authors would like to thank Dr. James Reed of DTRA for his support of this work.

[1]R. Waser, R. Dittmann, G. Staikov, and K. Szot, Adv. Mater. **21**, 2632–2663 (2009).
[2]J. J. Yang, D. B. Strukov, and D. R. Stewart, Nat. Nanotechnol. **8**, 13–24 (2013).
[3]H. -S. P. Wong, H. Lee, S. Yu, Y.-S. Chen, Y. Wu, P.-S. Chen, B. Lee, F. T. Chen, and M.-J. Tsai, Proc. IEEE **100**, 1951–1970 (2012).
[4]B. Govoreanu, G. S. Kar, Y. Chen, V. Paraschiv, S. Kubicek, A. Fantini, I. P. Radu, L. Goux, S. Clima, R. Degraeve, N. Jossart, O. Richard, T. Vandeweyer, K. Seo, P. Hendrickx, G. Pourtois, H. Bender, L. Altimime, D. J. Wouters, J. A. Kittl, and M. Jurczak, Tech. Dig. - Int. Electron Devices Meet. **2011**, 729–732.
[5]H. Y. Lee, Y. S. Chen, P. S. Chen, P. Y. Gu, Y. Y. Hsu, S. M. Wang, W. H. Liu, C. H. Tsai, S. S. Sheu, P. C. Chiang, W. P. Lin, C. H. Lin, W. S. Chen, F. T. Chen, C. H. Lien, and M.-J. Tsai, Tech. Dig. - Int. Electron Devices Meet. **2010**, 460–463.
[6]M.-F. Chang, C.-W. Wu, C.-C. Kuo, S.-J. Shen, K.-F. Lin, S.-M. Yang, Y.-C. King, C.-J. Lin, and Y.-D. Chih, Tech. Dig. - Int. Solid-State Circuits Conf. **2012**, 434–435.
[7]B. Gao, B. Sun, H. Zhang, L. Liu, X. Liu, R. Han, J. Kang, and B. Yu, IEEE Electron Device Lett. **30**, 1326–1328 (2009).
[8]X. Guan, S. Yu, and H. -S. P. Wong, IEEE Trans. Electron Devices **59**, 1172–1182, (2012).
[9]D. Ielmini, IEEE Trans. Electron Devices **58**, 4309–4317 (2011).
[10]S. Gerardin, M. Bagatin, A. Paccagnella, K. Grurmann, F. Gliem, T. R. Oldham, F. Irom, and D. N. Nguyen, IEEE Trans. Nucl. Sci. **60**, 1953–1969 (2013).
[11]W. M. Tong, J. J. Yang, P. J. Kuekes, D. R. Stewart, R. S. Williams, E. DeIonno, E. E. King, S. C. Witczak, M. D. Looper, and J. V. Osborn, IEEE Trans. Nucl. Sci. **57**, 1640–1643 (2010).
[12]H. J. Barnaby, S. Malley, M. Land, S. Charnicki, A. Kathuria, B. Wilkens, E. DeIonno, and W. M. Tong, IEEE Trans. Nucl. Sci. **58**, 2838–2844 (2011).
[13]E. DeIonno, M. D. Looper, J. V. Osborn, and J. W. Palko, IEEE Trans. Nucl. Sci. **60**, 1379–1383 (2013).
[14]E. DeIonno, M. D. Looper, J. V. Osborn, H. J. Barnaby, and W. M. Tong, IEEE Aerosp. Conf. **2013**, 1–8.
[15]M. J. Marinella, S. M. Dalton, P. R. Mickel, P. E. D. Dodd, M. R. Shaneyfelt, E. Bielejec, G. Vizkelethy, and P. G. Kotula, IEEE Trans. Nucl. Sci. **59**, 2987–2994 (2012).
[16]L. Zhang, R. Huang, D. Gao, P. Yue, P. Tang, F. Tan, Y. Cai, and Y. Y. Wang, IEEE Trans. Electron Devices **58**, 2800–2804 (2011).
[17]F. Tan, R. Huang, X. An, Y. Cai, Y. Pan, W. Wu, H. Feng, X. Zhang, and Y. Y. Wang, IEEE Trans. Nucl. Sci. **60**, 4520–4525 (2013).
[18]X. He and R. E. Geer, IEEE Aerosp. Conf. **2013**, 1–7.
[19]J. S. Bi, Z. S. Han, E. X. Zhang, M. W. McCurdy, R. A. Reed, R. D. Schrimpf, D. M. Fleetwood, M. L. Alles, R. A. Weller, D. Linten, M. Jurczak, and A. Fantini, IEEE Trans. Nucl. Sci. **60**, 4540–4546 (2013).

[20]Y. Gonzalez-Velo, H. J. Barnaby, M. N. Kozicki, P. Dandamudi, A. Chandran, K. E. Holbert, M. Mitkova, and M. Ailavajhala, IEEE Trans. Nucl. Sci. **60**, 4563–4569 (2013).
[21]B. Butcher, X. He, M. Huang, Y. Wang, Q. Liu, H. Lv, M. Liu, and W. Wang, Nanotechnology **21**, 475206 (2010).
[22]Y. Wang, H. Lv, W. Wang, Q. Liu, S. Long, Q. Wang, Z. Huo, S. Zhang, Y. Li, Q. Zuo, W. Lian, J. Yang, and M. Liu, IEEE Electron Device Lett. **31**, 1470–1472 (2010).
[23]U. S. Joshi, S. J. Trivedi, K. H. Bhavsar, U. N. Trivedi, S. A. Khan, and D. K. Avasthi, J. Appl. Phys. **105**, 073704 (2009).
[24]S. Yu, Y. Wu, Y. Chai, J. Provine, and H. -S. P. Wong, Int. Symp. VLSI-TSA **2011**, 106–107.
[25]J.-C. Dupin, D. Gonbeau, P. Vinatier, and A. Levasseur, Phys. Chem. Chem. Phys. **2**, 1319–1324 (2000).
[26]Y. S. Lin, F. Zeng, S. G. Tang, H. Y. Liu, C. Chen, S. Gao, Y. G. Wang, and F. Pan, J. Appl. Phys. **113**, 064510 (2013).